THE OHIO STATE UNIVERSITY

Stall Cell Formation on a Boeing Vertol VR-7 Airfoil

Ata Esfahani †, Nathan Webb and Mo Samimy

Gas Dynamics and Turbulence Laboratory (GDTL)
Aerospace Research Center
The Ohio State University

55th AIAA Aerospace Sciences Meeting
Grapevine, TX, 9-13 Jan 2017

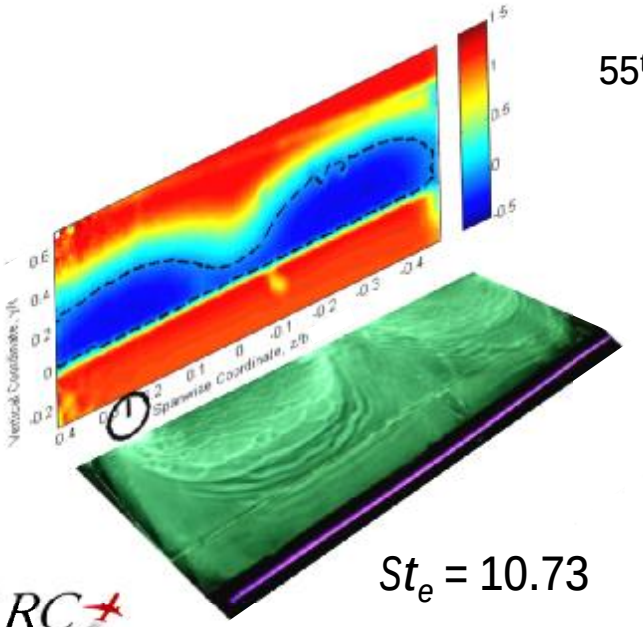

St_e = 10.73

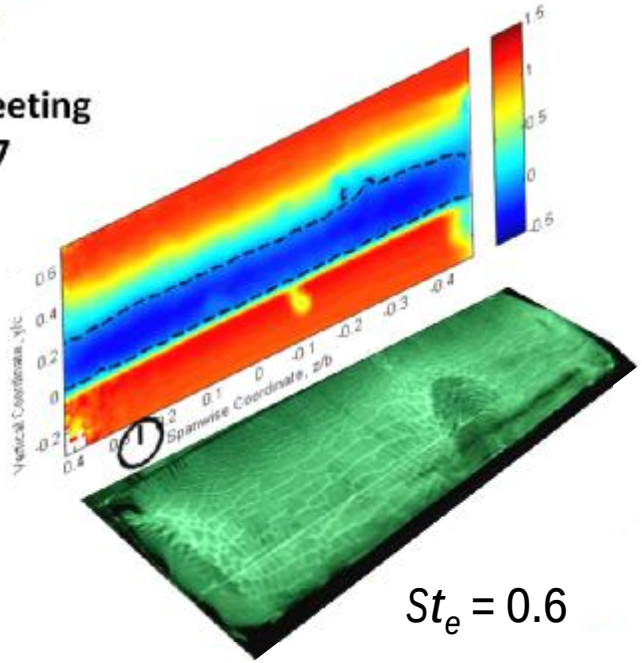

St_e = 0.6

ARC

Outline

- Previous Work/Background
- Motivation/Introduction
- Experimental Setup
- Results
  - Surface Topology (Fluorescent Surface Oil Flow Visualization)
  - Velocity Distribution (2D-2C and Stereo PIV)
- Hypothesis
- Conclusions

Our Previous Work:
Low and High-Freq. Flow Excitation with NS-DBD Actuators

- Large-scale, coherent structures are generated due to low-frequency excitation ($St_e < 2$).
- Vortex shedding leads to shear layer flapping and unsteady loads
- High-frequency excitation ($St_e > 6$) results in formation of small-scale structures that develop and disintegrate quickly.
- Shear layer flapping is absent at high-frequency excitation regimes. Therefore, the airfoil does not experience unsteady loads
- We observed discrepancy between PIV and pressure data obtained at different spanwise locations → *3D flow?*

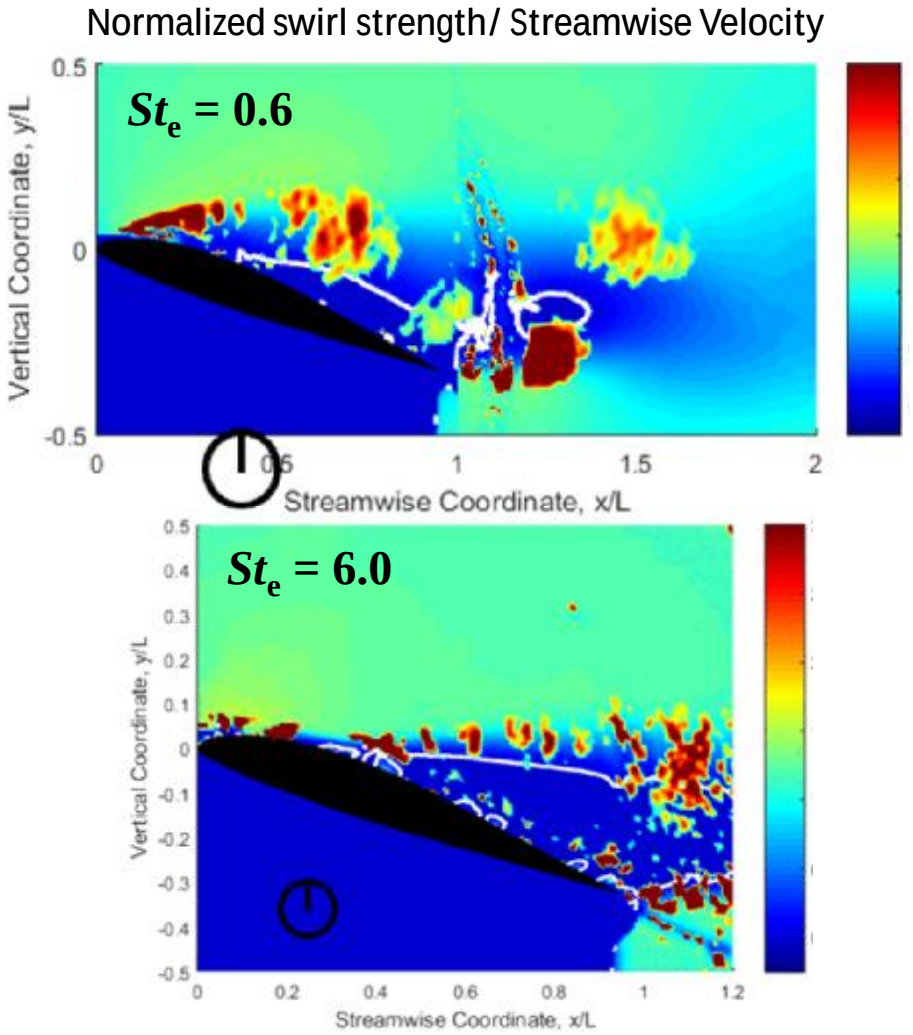

Esfahani, A., Singhal, A., Clifford, C. J., and Samimy, M., "Flow Separation Control over a Boeing Vertol VR-7 using NS-DBD Plasma Actuators", AIAA paper 2016-0843

Background:
Stall Cell Formation and Structure

- Crow instability is believed to be the possible mechanism leading to t
- A complex vortex syste cells are formed
- Streamwise vortices layer bend the shear edge of the cells

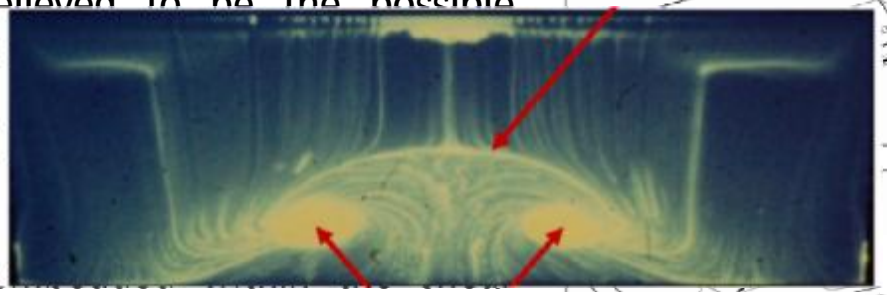

Surface oil flow visualization of a single stall cell[1]

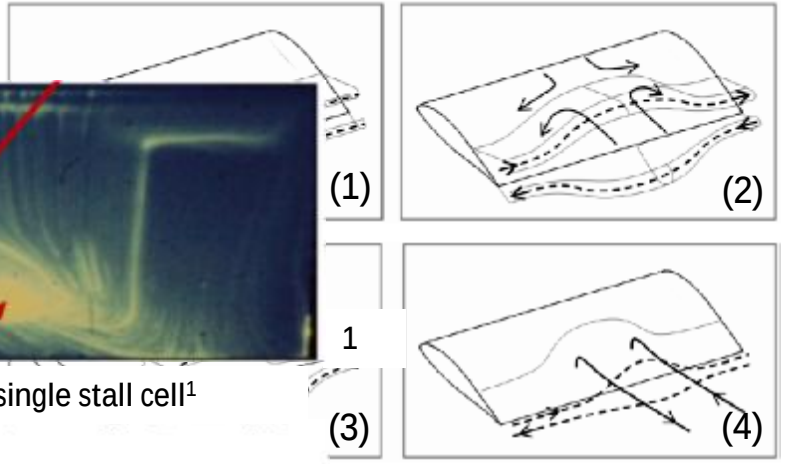

1

e formation of stall cells[2]

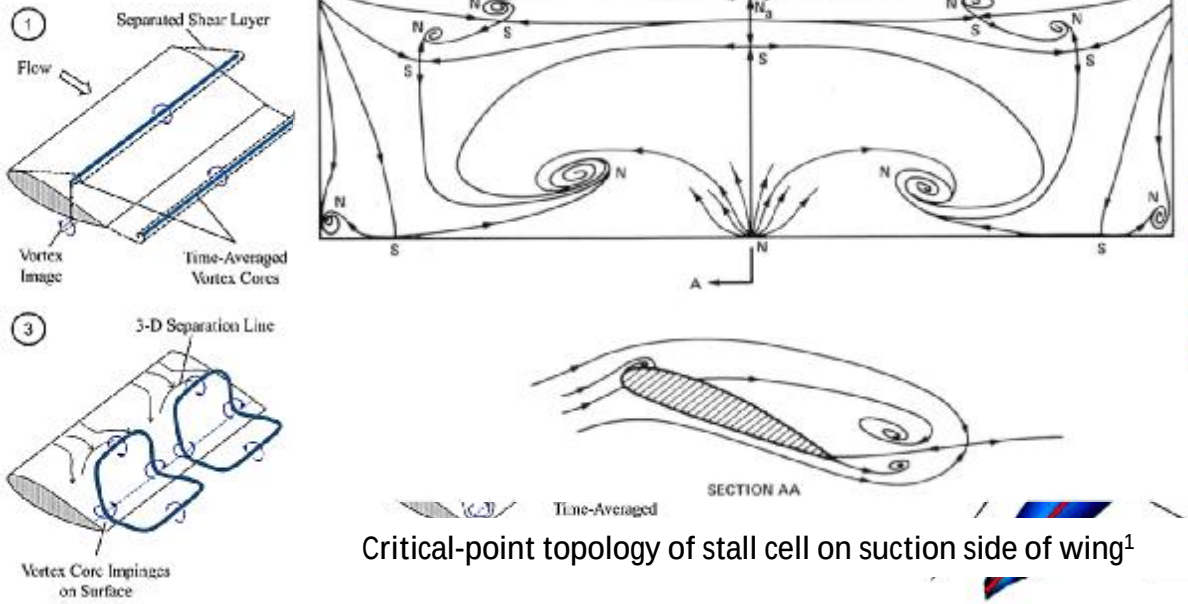

Critical-point topology of stall cell on suction side of wing[1]

Crow instability model for stall cell formation[1]

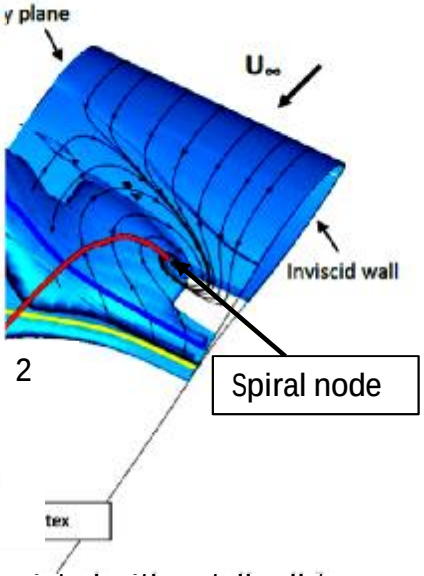

2

Vortex system associated with a stall cell [2]

1. Courtesy of Prof. Allen E. Winkelmann
2. Peake and Tobak, NASA Technical Memorandum
1. Weihs and Katz, AIAA J, 1983
2. M. Manolesos, PhD thesis, 2013

Motivation:
Consequences of Stall Cell Formation

- Emergence of stall cells results in significant changes in lift and drag coefficients.
- Stall cells also induce spanwise variations in sectional loads which is highly undesirable.
- Results obtained from 2D measurements are no longer representative of the entire flow field, hence, 3D flow diagnostics techniques are needed.

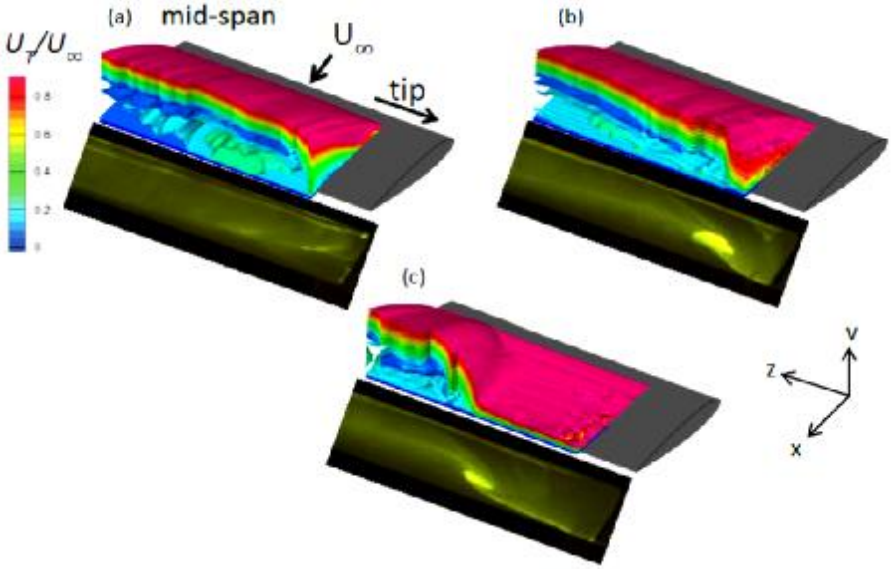

Spanwise variations in separation height in the presence of stall cells over a NACA 0015 airfoil at different Reynolds numbers[3]

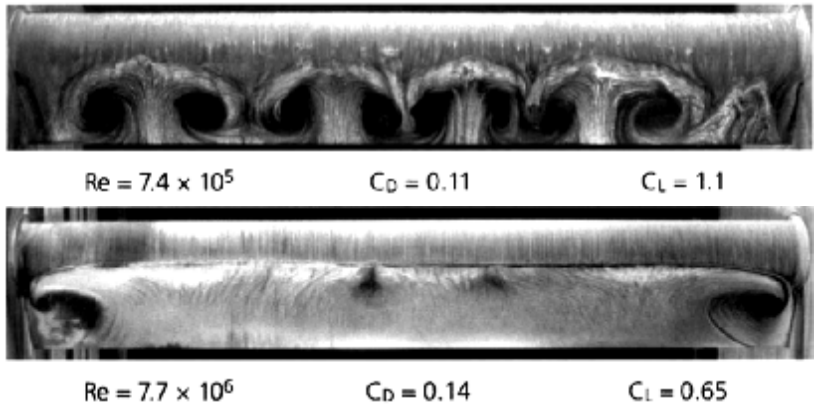

Stall Cell formation on thick, AR=6 wing at various Reynolds numbers[1]

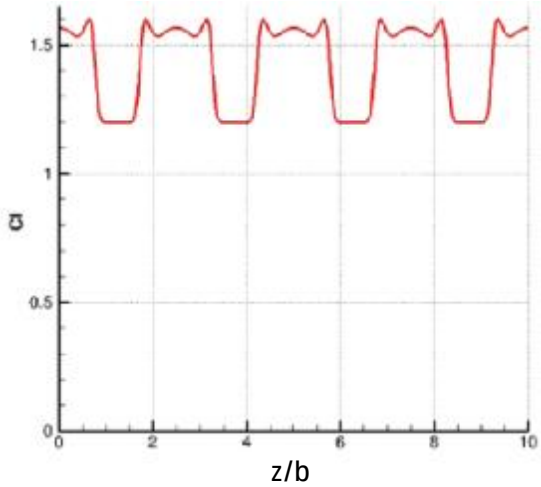

Distribution of sectional lift on an infinite wing due to the presence of stall cell[2]

1. Schewe, Journal of wind engineering, (89), pp1267-1289, 2001
2. Spalart, AIAA journal, 2014
3. De Mauro et al. AIAA paper 2015-2633

Introduction:
Affecting Stall Cell Patterns via Spanwise Perturbations

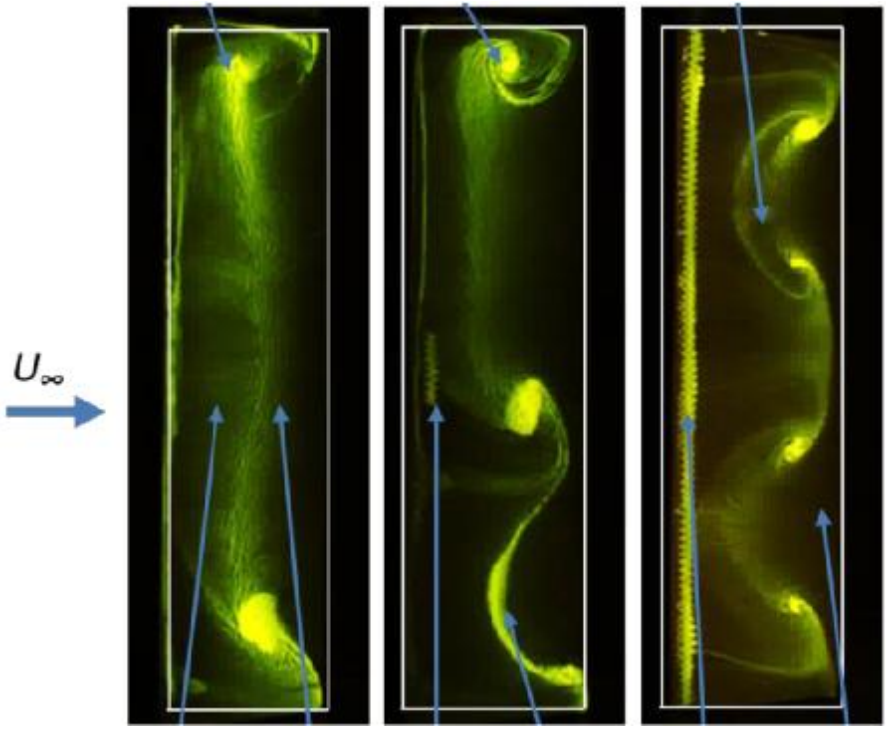

Perturbing cross-flow instabilities by zig-zag tapes of various lengths and heights on a NACA 0015 airfoil at **α**=16 at Re=340,000 (Amitay group, RPI)[1]

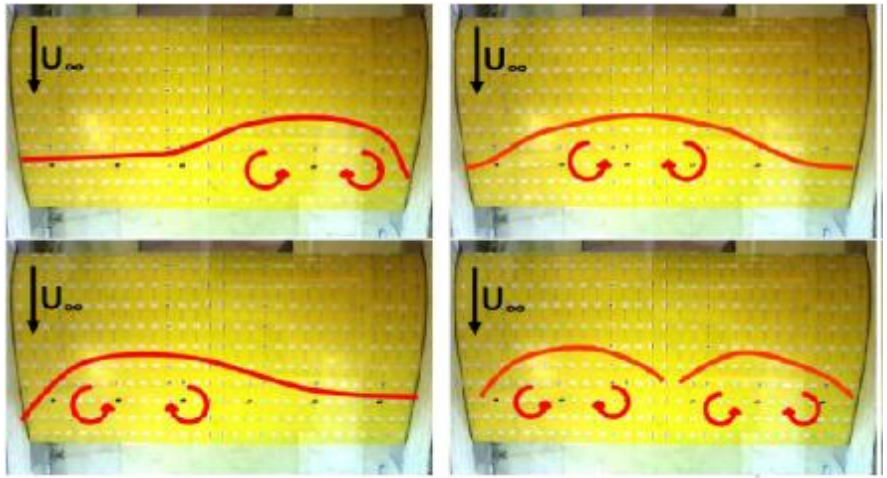

Unstable nature of SCs without zig-zag tape. AR 2.0, a = 11 °, Re = 1.0×10^6 [2]

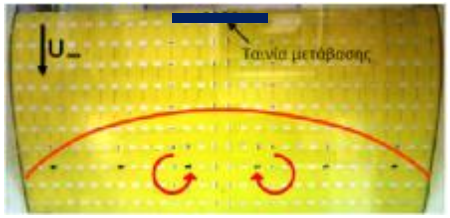

Single stable SC with a 10% span zig-zag tape[2]

- Spanwise perturbations have shown to be effective in inducing stall cells and affecting their patterns
- The role of spanwise perturbations created by NS-DBD actuators in inducing stall cells is investigated in our work.

1. V. Sivaneri, MSc Thesis, Rensselaer Polytechnic, 2014
2. M. Manolesos, PhD thesis, 2013

Outline

- Previous Work/Background
- Motivation/Introduction
- Experimental Setup
- Results
  - Surface Topology (Fluorescent Surface Oil Flow Visualization)
  - Velocity Distribution (2D-2C and Stereo PIV)
- Hypothesis
- Conclusions

Wind Tunnel:

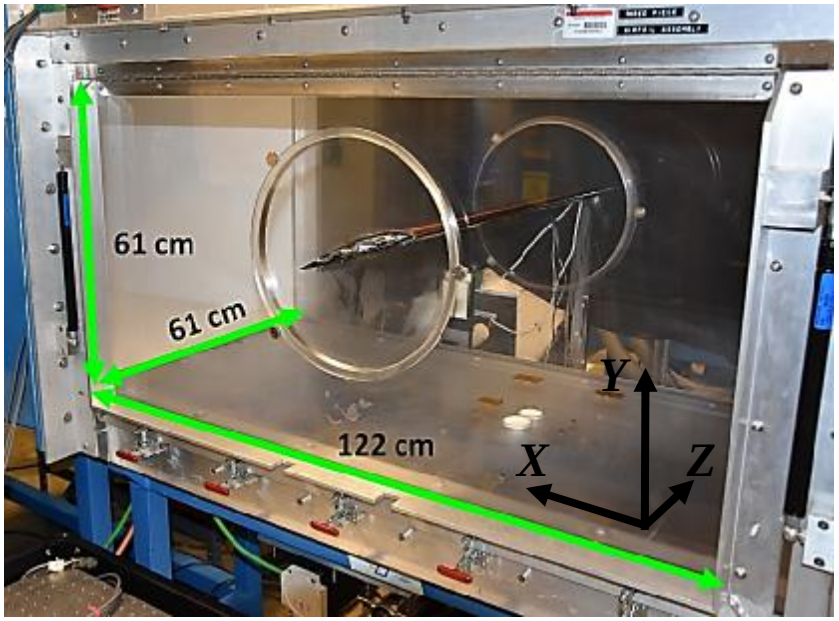

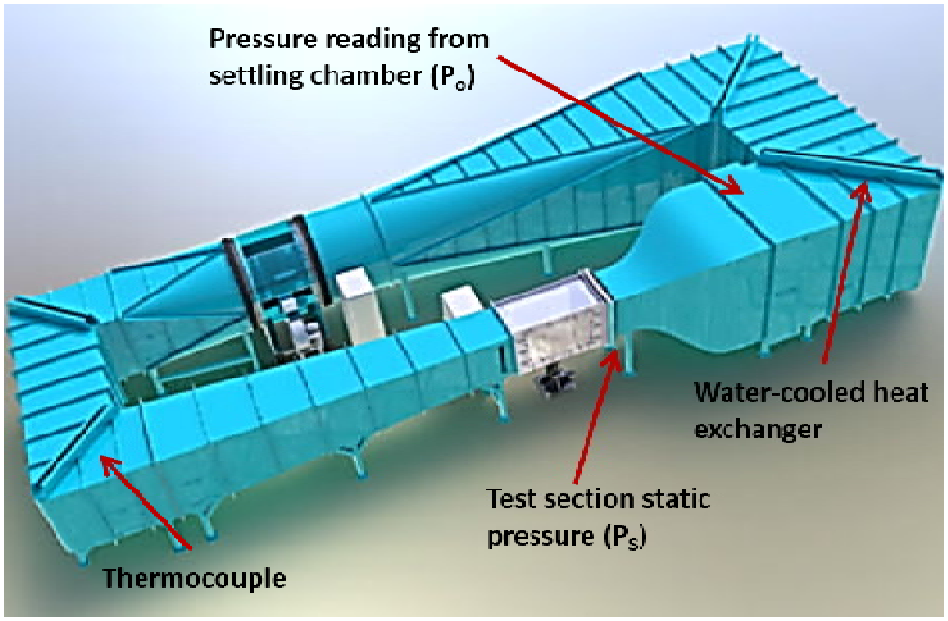

Closed circuit, temperature-controlled wind tunnel

- Freestream turbulence intensity of 0.25%
- $Re_c = 0.2 \times 10^6 - 1.1 \times 10^6$
- U_∞ = 10 - 90 m/s
- Manually and automatically adjustable angle of attack

Test Conditions

- $Re = \mathbf{0.5 \times 10^6}$
- $\boldsymbol{U_\infty}$ = 38 m/s
- $\boldsymbol{\alpha}$ = 19° (deep post-stall AOA)

Airfoil and Coordinates:

$$St_e = \frac{f_e c}{U_\infty}$$

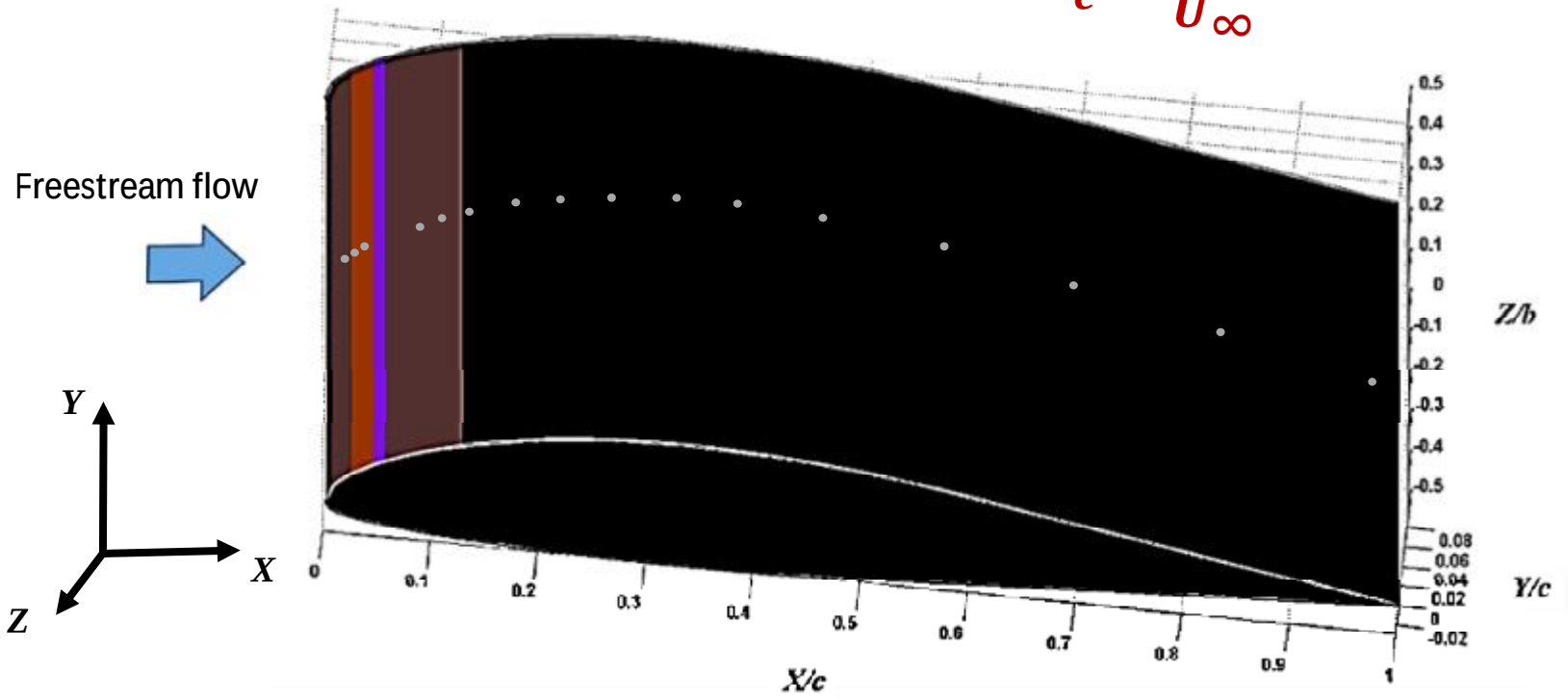

- Airfoil: VR-7 rotorcraft blade, made of non-conductive fiberglass composite with built-in actuator recess
- Maximum thickness: 10% of chord
- Chord length $c = 20.3\,cm$, mounted in the center of test section between two acrylic disks
- 16 pressure taps on the suction side
- 17 pressure taps on the pressure side

NS-DBD Actuator and Pulser:

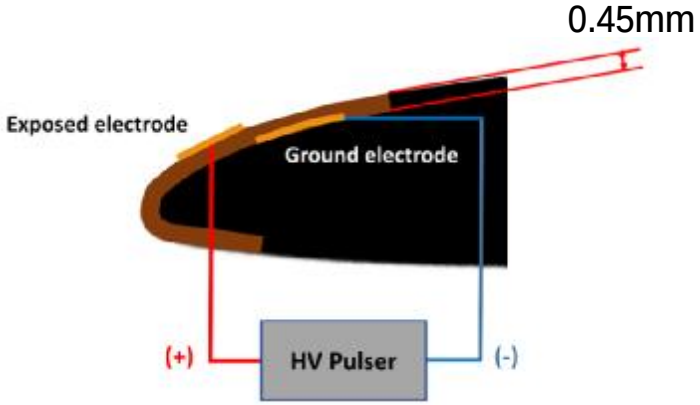

- The pulser generates high-voltage (~ 10 kV) high-repetition rate pulses (100 Hz- 10 kHz) through magnetic wave compression that are approximately 50 ns wide at FWHM
- The energy input by the pulser is 18 mJ per pulse
- The barrier discharge created between copper electrodes, generates thermal perturbations that excite the flow instabilities
- It is not clear whether the thermal perturbations or the compression waves are responsible for exciting the instabilities

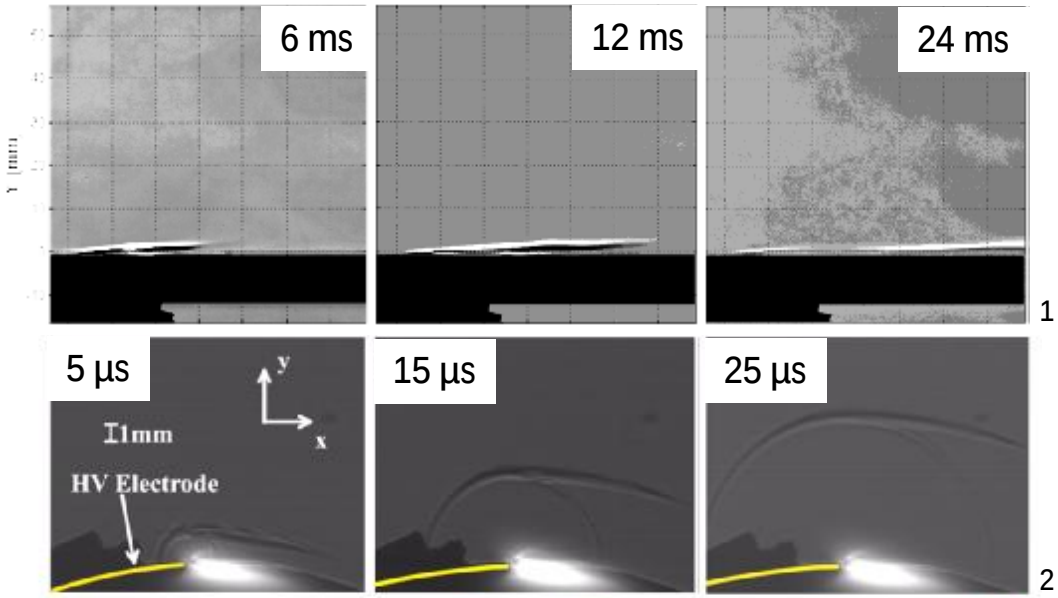

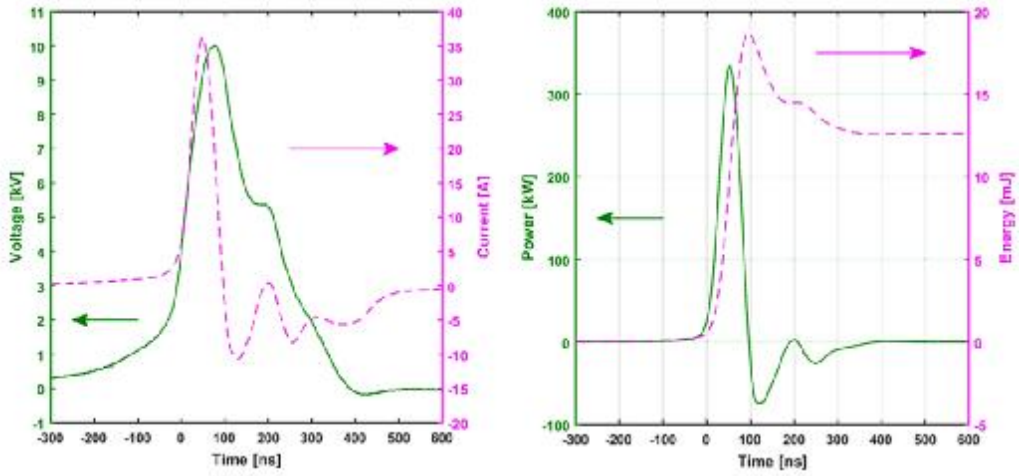

Samples traces of current and voltage and input power and energy per pulse

1. Correale et al. J Phys. D: Appl. Phys. (47) 2014
2. Little et al. AIAAJ 50 (2) Feb 2012

Fluorescent SOFV Setup:

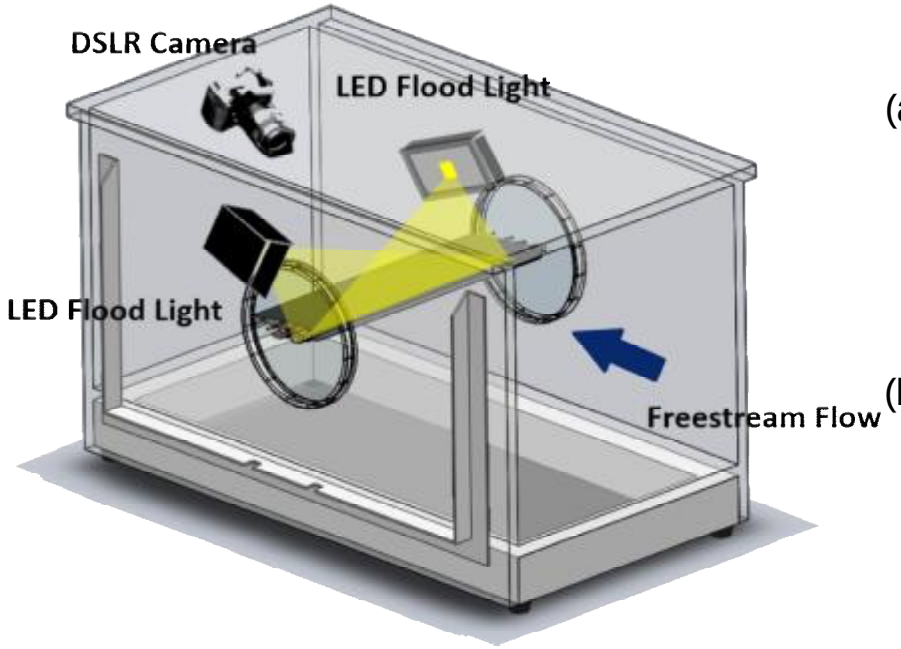

- 32 MP Nikon DSLR camera with 18-300 mm variable focal length lens
- 2 x 100 W white LED arrays
- Mixture of 350 cSt & 10,000 cSt silicone oil at 5,000 cSt
- 35 µm uncoated fluorescent pigments

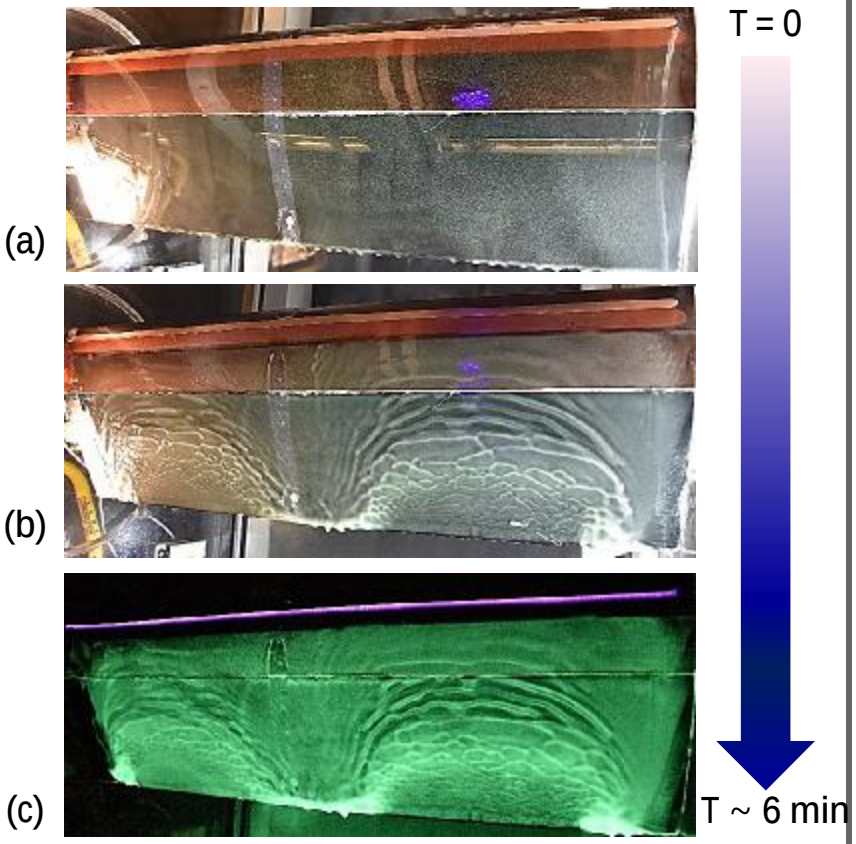

(a) Model covered with a thin sheet of oil in quiescent flow conditions (b) Illuminated model once steady flow is established (c) Fluorescence emissions in the dark lab

2D-2C PIV Setup:

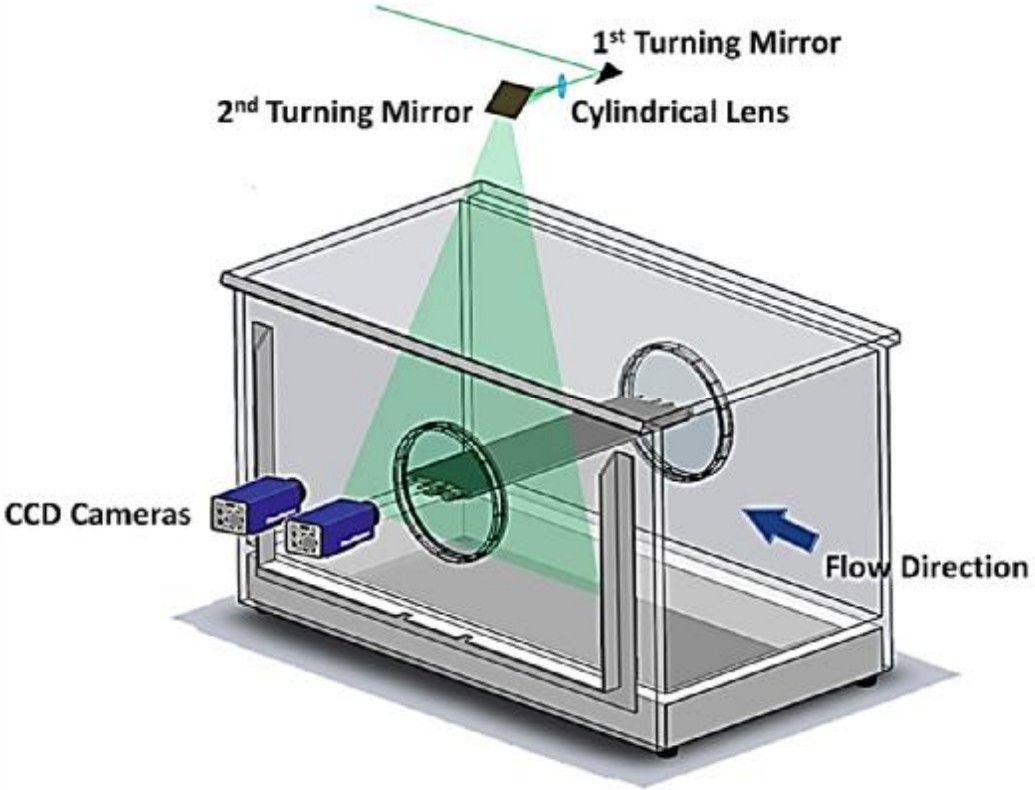

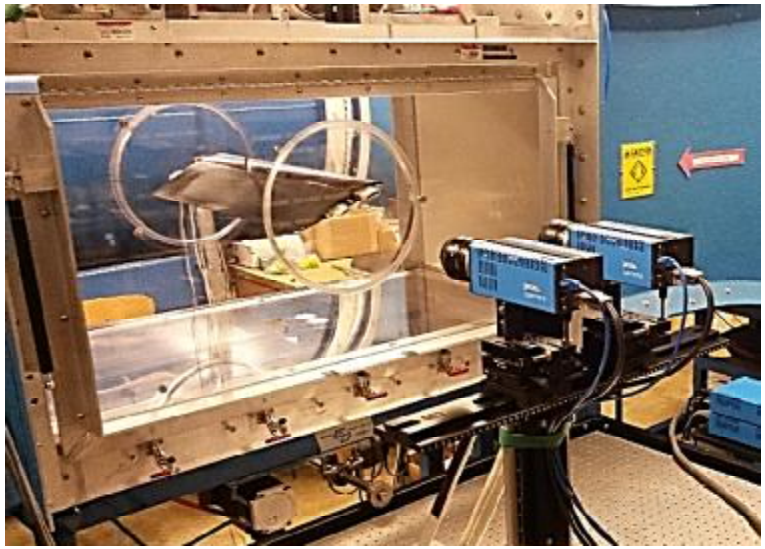

- Streamwise two-component PIV (ensemble-averaged)
- Nd:YAG dual-head 532 nm laser providing forward scattering
- Two 4 MP 14-bit dual-frame Imager Pro X CCD cameras capable of acquiring images at 10 Hz
- 500 images acquired for each data point. Images are then stitched together to obtain the flow field over the airfoil and in the wake

2D-2C PIV Data Sample (St_e = 0.6):

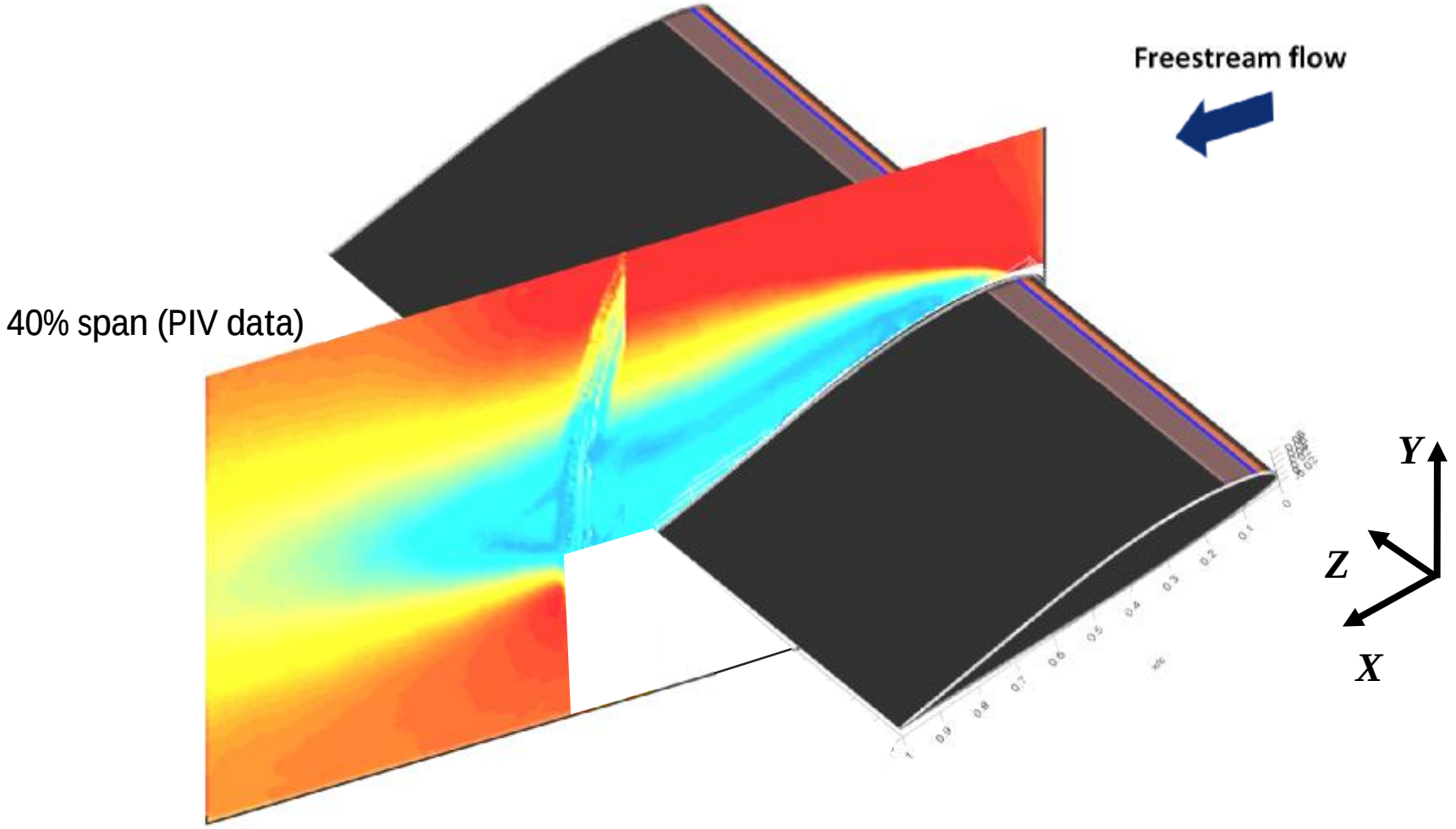

- All of 2D-2C data are acquired at 40% span (*z/b = -0.1)* due to optical access restrictions

Stereo PIV Setup:

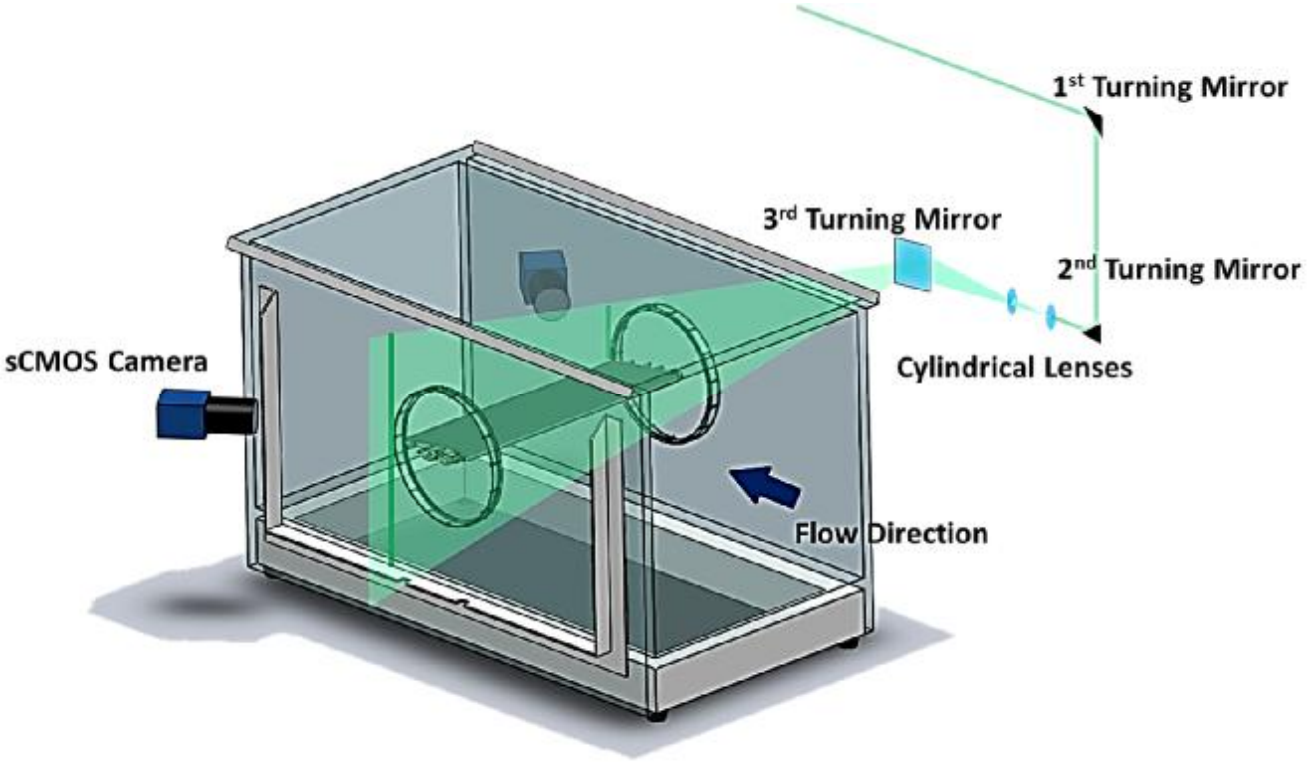

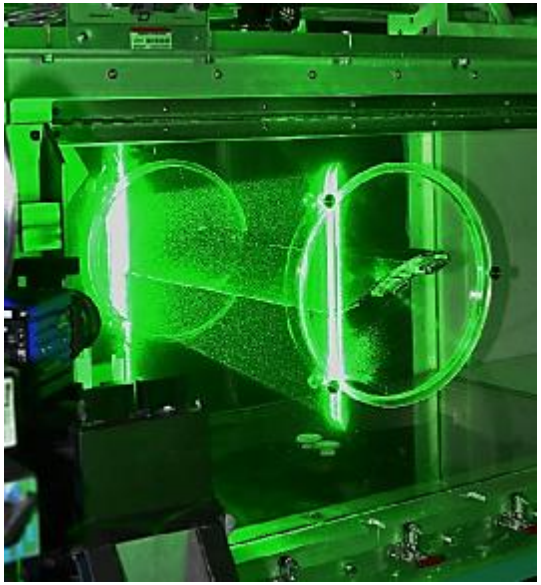

- Spanwise three-component stereo PIV (ensemble-averaged)
- Nd:YAG dual-head 532 nm laser providing forward and backward scattering
- Two 5 MP 16-bit dual-frame sCMOS cameras capable of acquiring images at 50 Hz
- 600 images acquired for each data point.
- Field of view covers 87% of the span

Stereo PIV Data Sample (St_e = 10.73):

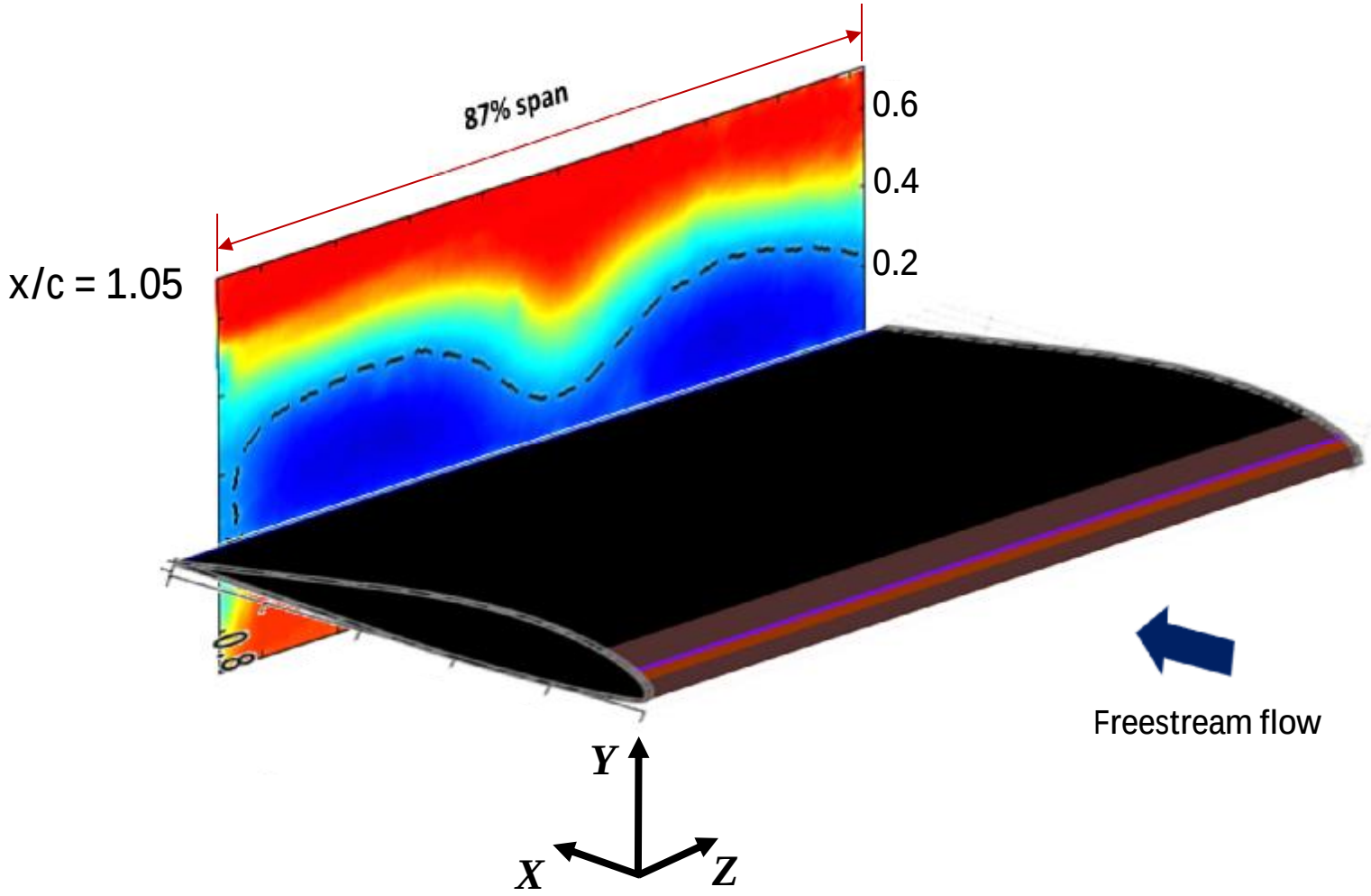

- All of stereo PIV data are acquired downstream of the trailing edge at *x/c = 1.05*

Outline

- Previous Work/Background
- Motivation /Introduction
- Experimental Setup
- Results
  - Surface Topology (Fluorescent Surface Oil Flow Visualization)
  - Velocity Distribution (2D-2C and Stereo PIV)
- Hypothesis
- Conclusions

Surface Topology: Low-Freq. Excitation Effects

Surface pressure and PIV data agree reasonably

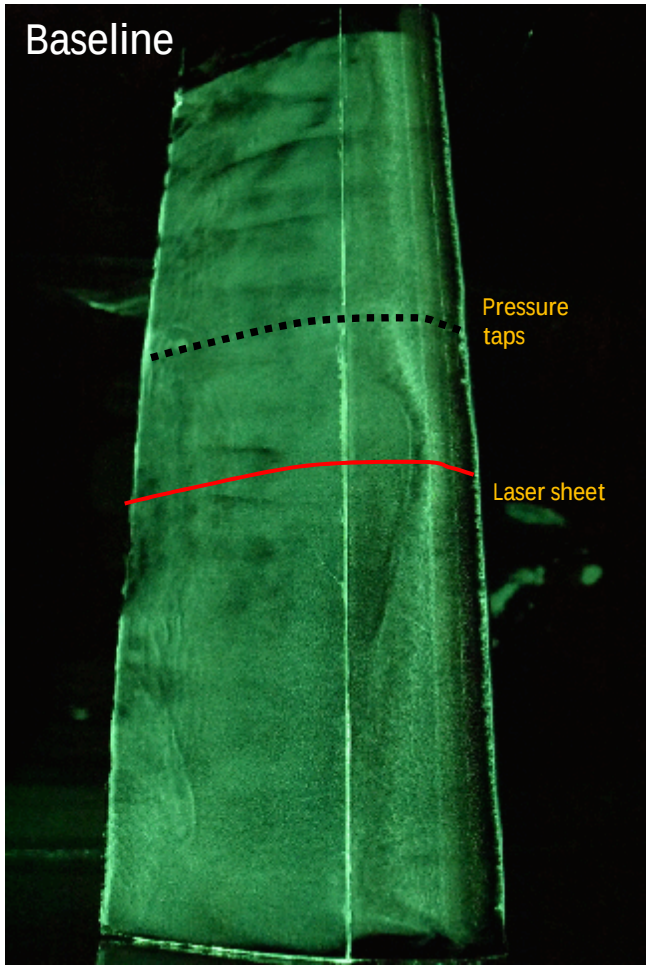

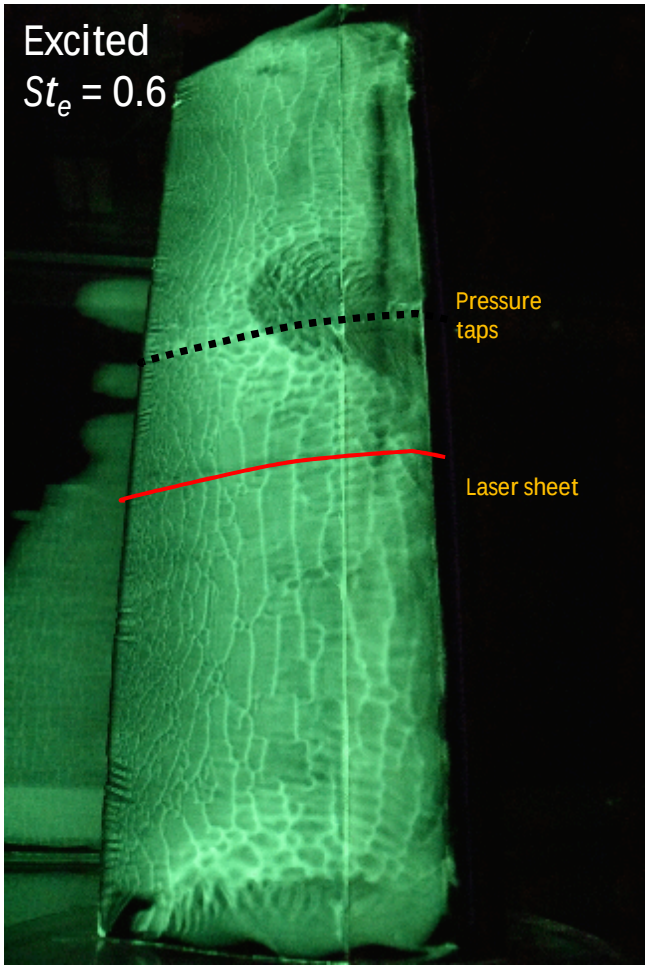

Freestream Flow

Surface pressure and PIV data DO NOT agree

- Excitation at St_e = 0.6 leads to the formation of an asymmetrical flow pattern
- The accelerated flow region is located on top of the pressure taps whereas the separated flow region falls under the laser sheet

Surface Topology: High-Freq. Excitation Effects

Surface pressure and PIV data agree reasonably

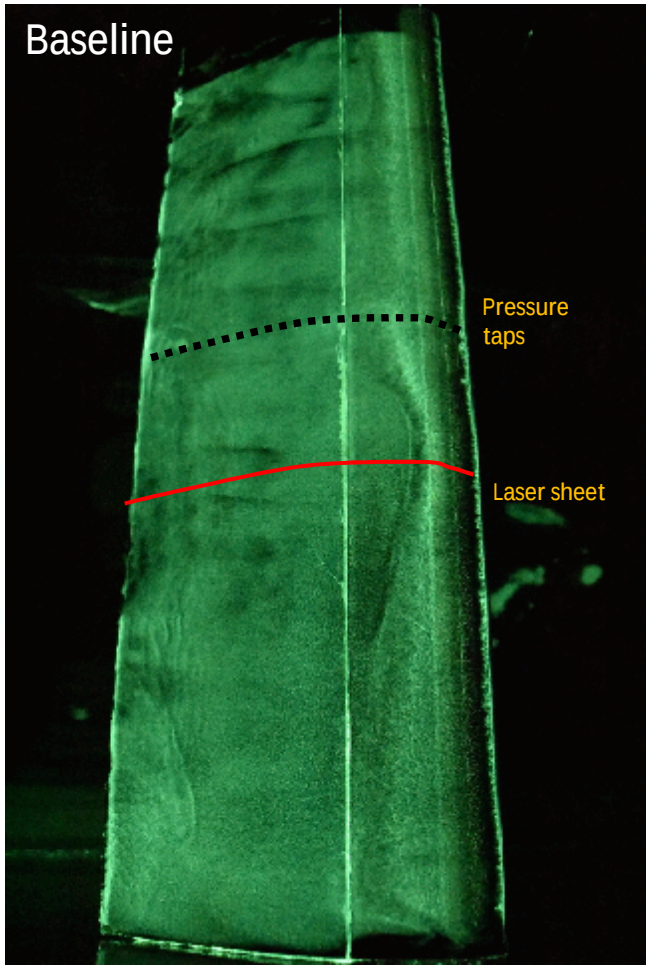

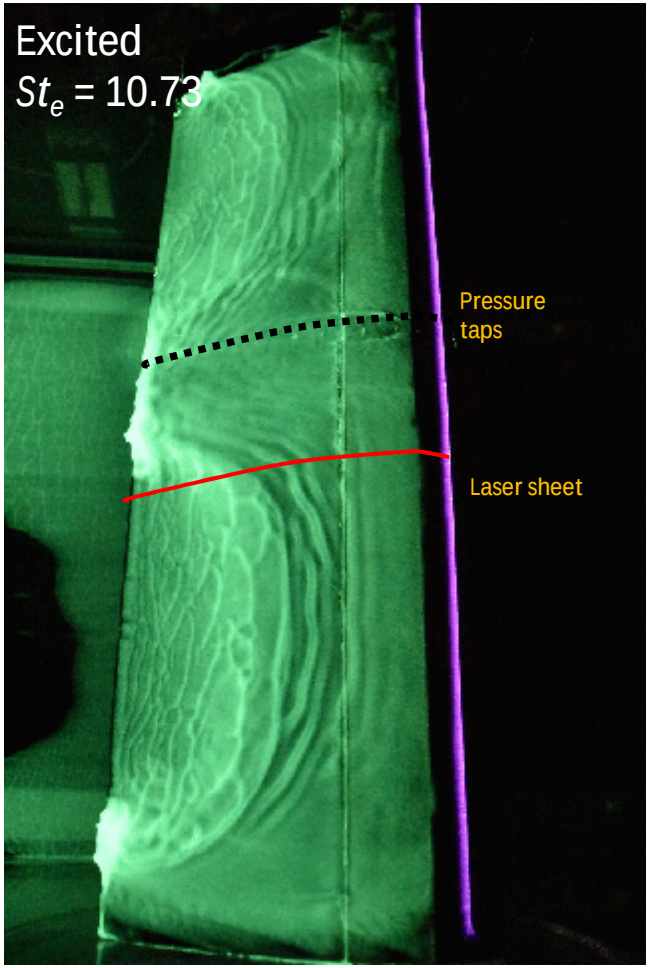

Freestream Flow

Surface pressure and PIV data DO NOT agree

- Excitation at St_e = 10.73 pushes the separation line further downstream and generates two, asymmetrical small cells.
- Stall cell wavelength and spacing does not agree with the existing correlations and formulae for thick airfoils

Surface Topology – Stereo PIV: Low-Freq. Excitation Effects

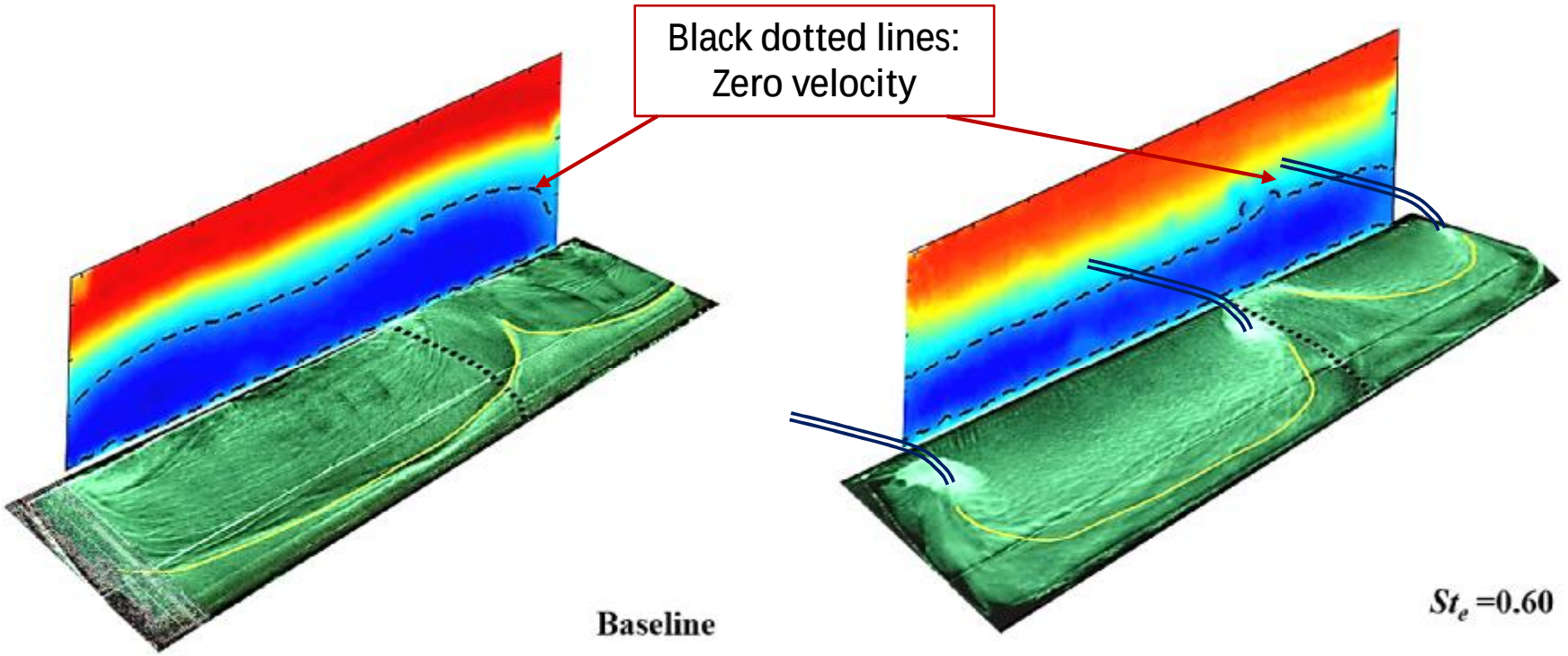

- Pressure taps fall outside the stall cells
- 3D separation front develops into two well-defined, asymmetric cells
- The strong streamwise vortices impinging on the surface do not bend the shear layer, possibly due to interaction with strong spanwise vortices generated by low-freq. excitation
- The presence of stall cells close to LE leads to major loss of lift as the majority of lift is generated at LE

Surface Topology – Stereo PIV: High-Freq. Excitation Effects

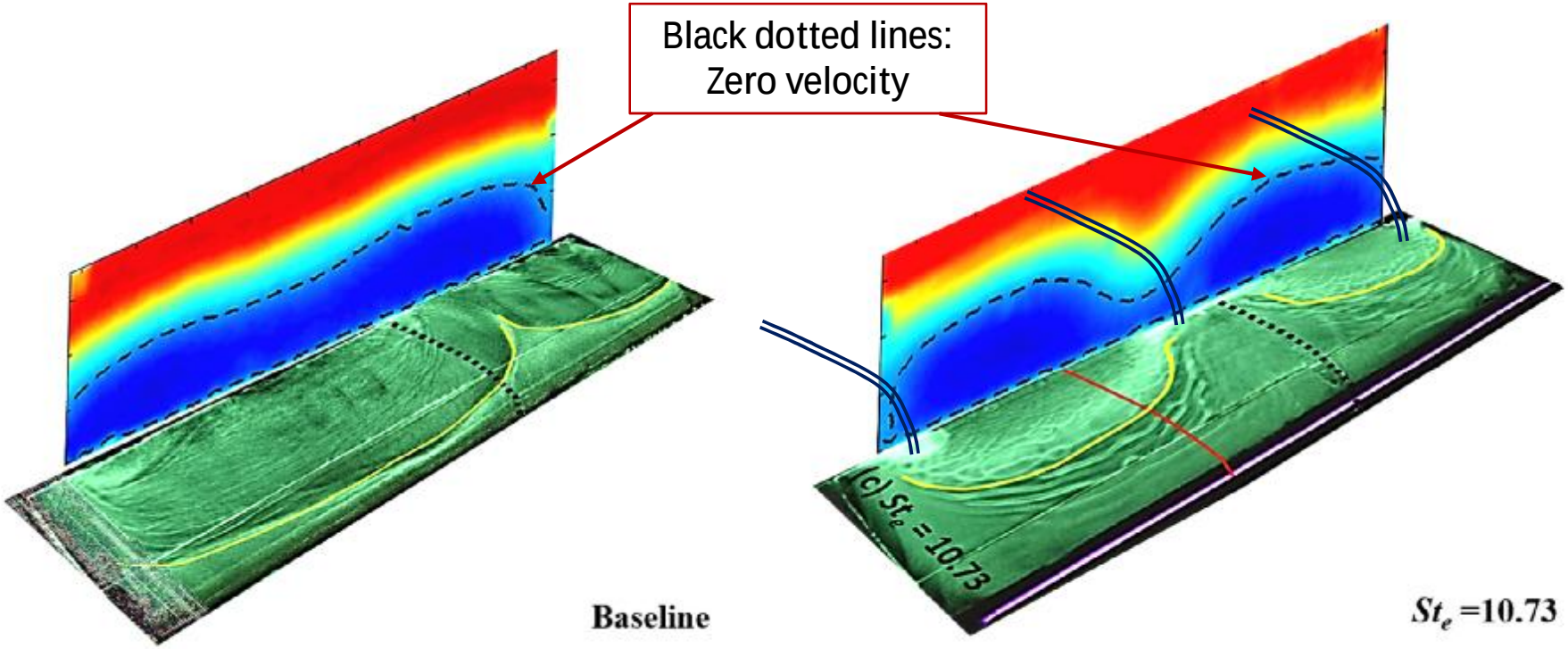

- Asymmetrical pattern is formed under high-freq. excitation
- Stall cells do not cover the pressure taps as was the case in low-freq. excitation
- Strongest streamwise vortices that bend the shear layer are seen on the right half of the model
- The bulk of the lift is generated close to LE, so the presence of stall cells close to TE will not induce major spanwise variations in loads

Outline

- Previous Work/Background
- Motivation /Introduction
- Experimental Setup
- Results
  - Surface Topology (Fluorescent Surface Oil Flow Visualization)
  - Velocity Distribution (2D-2C and Stereo PIV)
- Hypothesis
- Conclusions

Ensemble-Averaged 2D-2C PIV: Comparison with Stereo PIV at Different Excitation Regimes

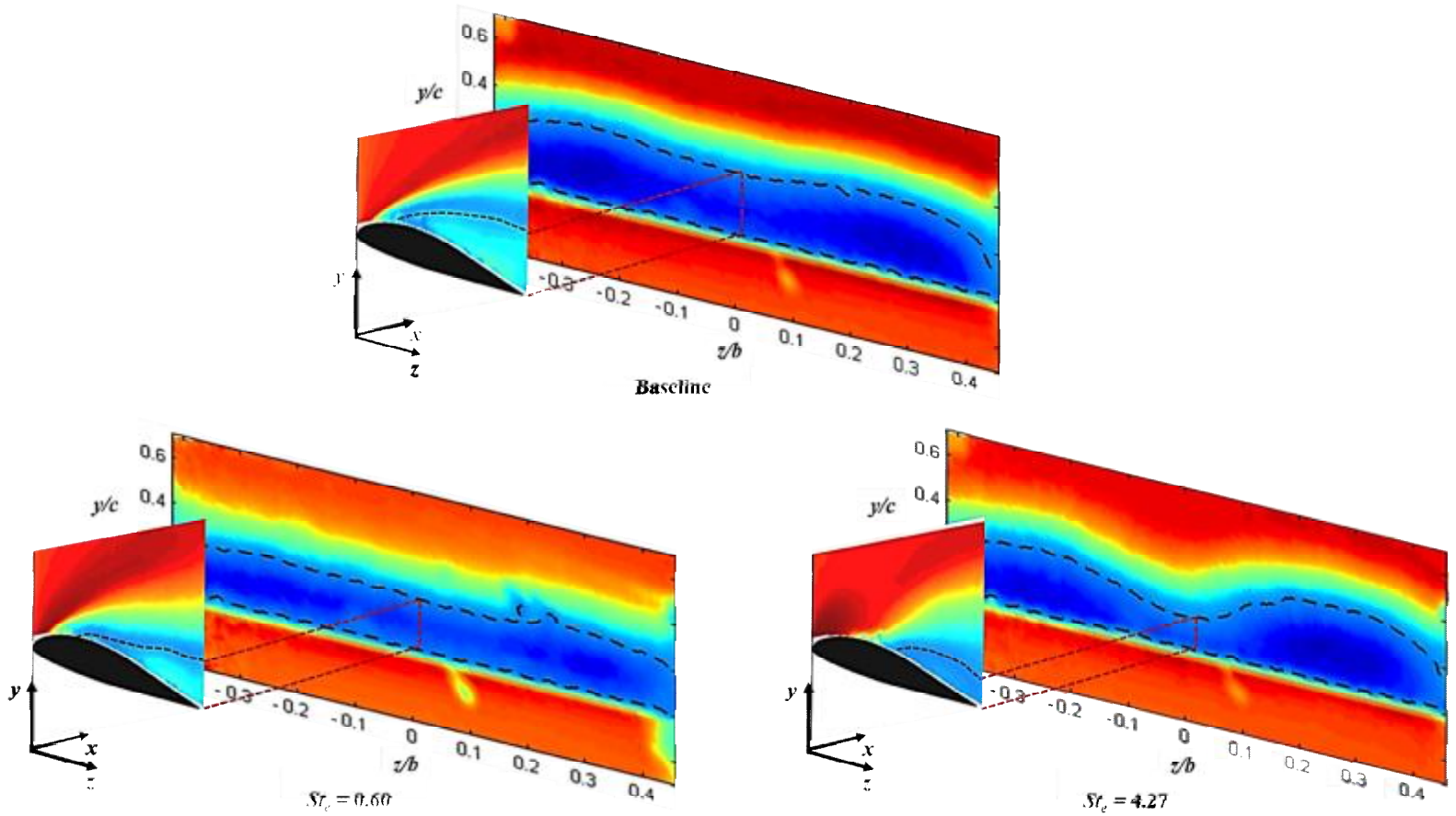

- 2D-2C data indicate that the separation height is reduced as the excitation freq. is increased but the opposite is true for stall cell height
- Calculating lift and drag using velocity distributions obtained from 2D data while the stall cells are present will lead to major errors

Ensemble-Averaged Stereo PIV ($\frac{u}{U_\infty}$): Low to High-Freq. Excitation Effects

- Low-frequency excitation nearly eliminates three-dimensionalities in the flow
- Better mixing across the shear layer is observed due to low-freq. excitation
- The geometry of the stall cells formed due to high-freq. excitation remains nearly invariant as the frequency is increased
- The streamwise vortices become stronger with high-freq. excitation and bend the shear layer
- Mixing across the shear layer is deteriorated at higher excitation frequencies

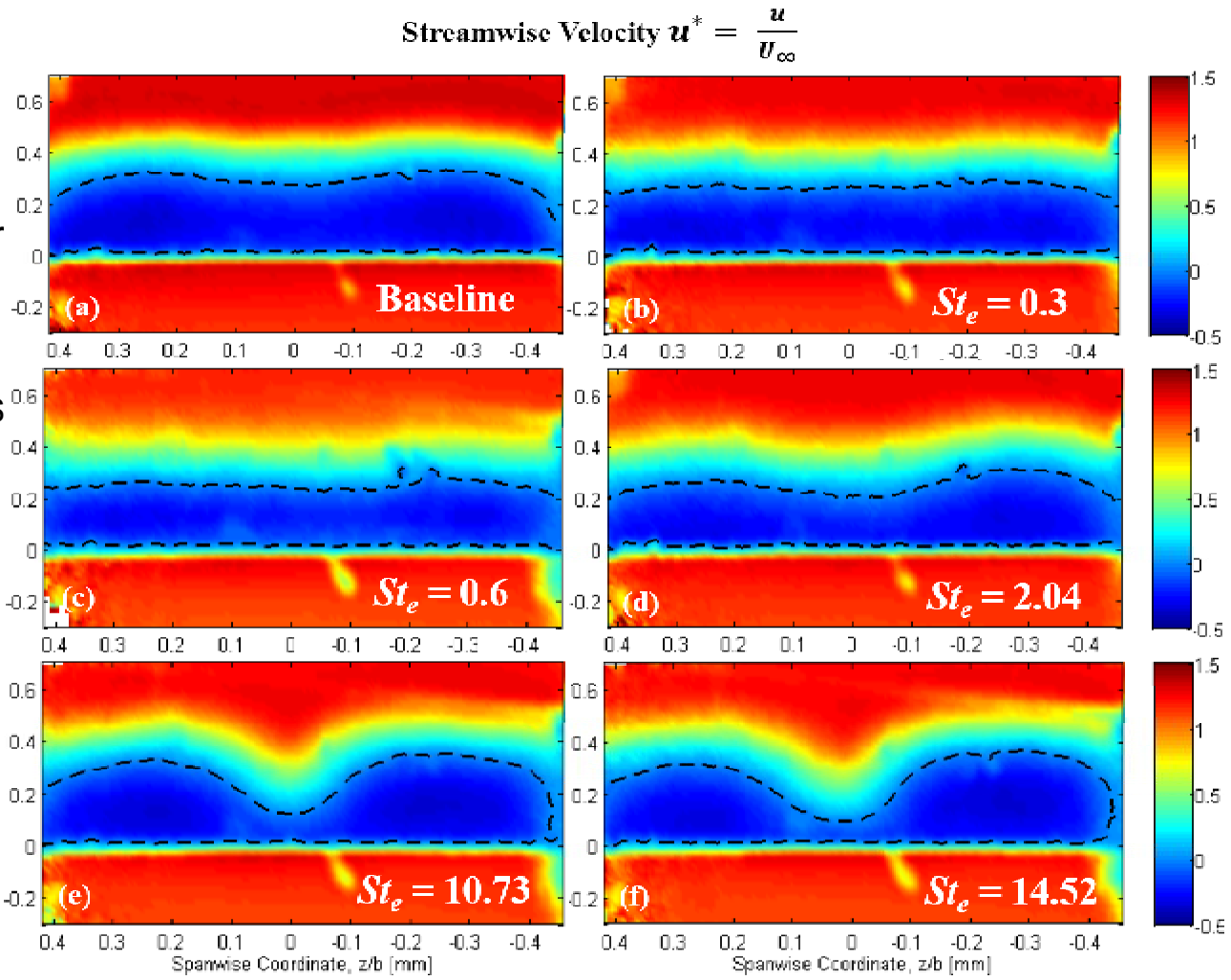

Ensemble-Averaged Stereo PIV ($\frac{v}{U_\infty}$): Low to High-Freq. Excitation Effects

- Low-frequency excitation generates strong spanwise-uniform shedding
- The strength of the vortices shed at the TE is reduced as the excitation frequency is increased and 3D features begin to emerge
- In-plane components of velocity indicate the presence of strong streamwise vortices at high excitation frequencies

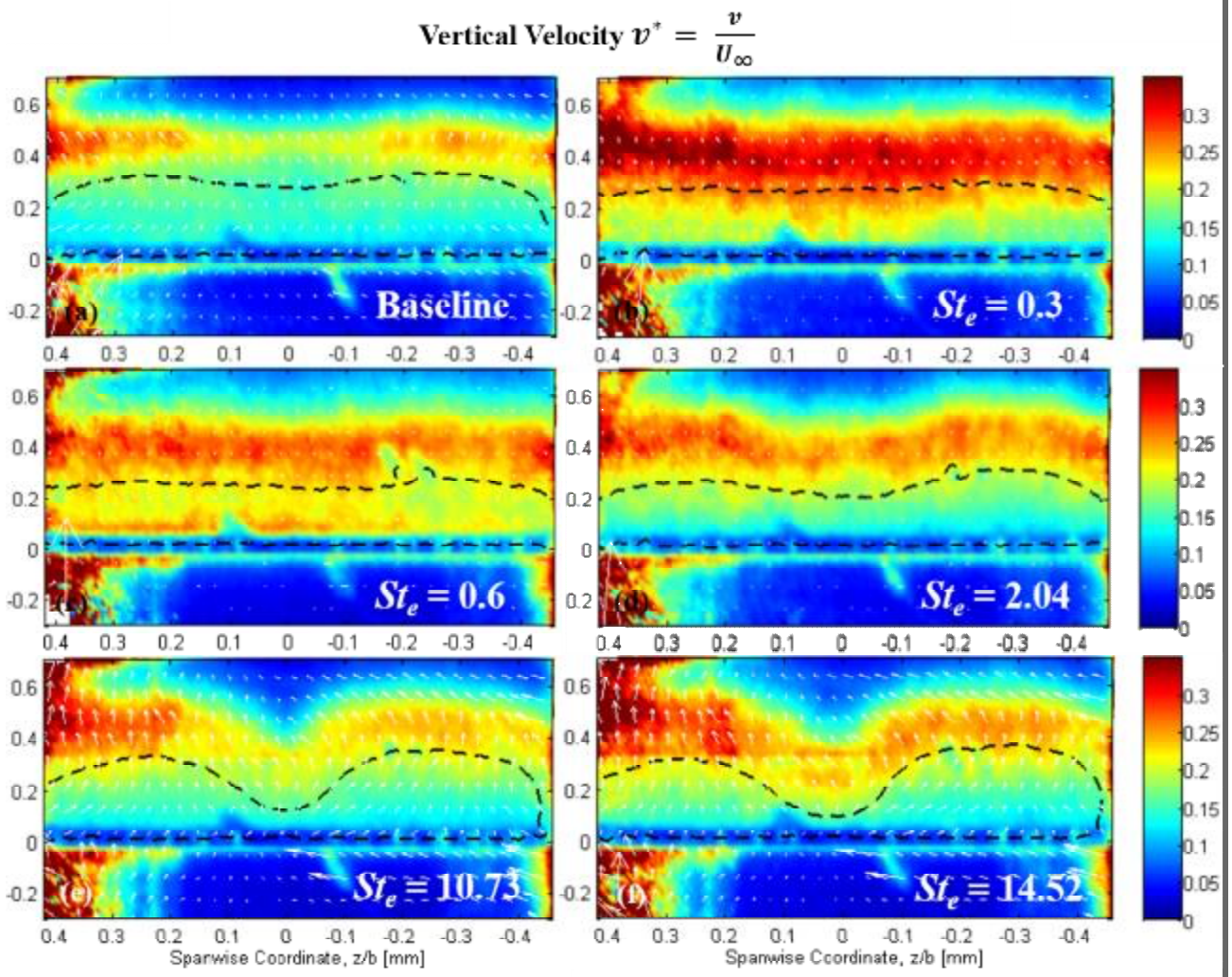

Ensemble-Averaged Stereo PIV ($\frac{u}{U_\infty}$) and ($\frac{v}{U_\infty}$):

THE OHIO STATE UNIVERSITY

Low-Freq. Modulation of *2 kHz* (St_e = 12) waveform

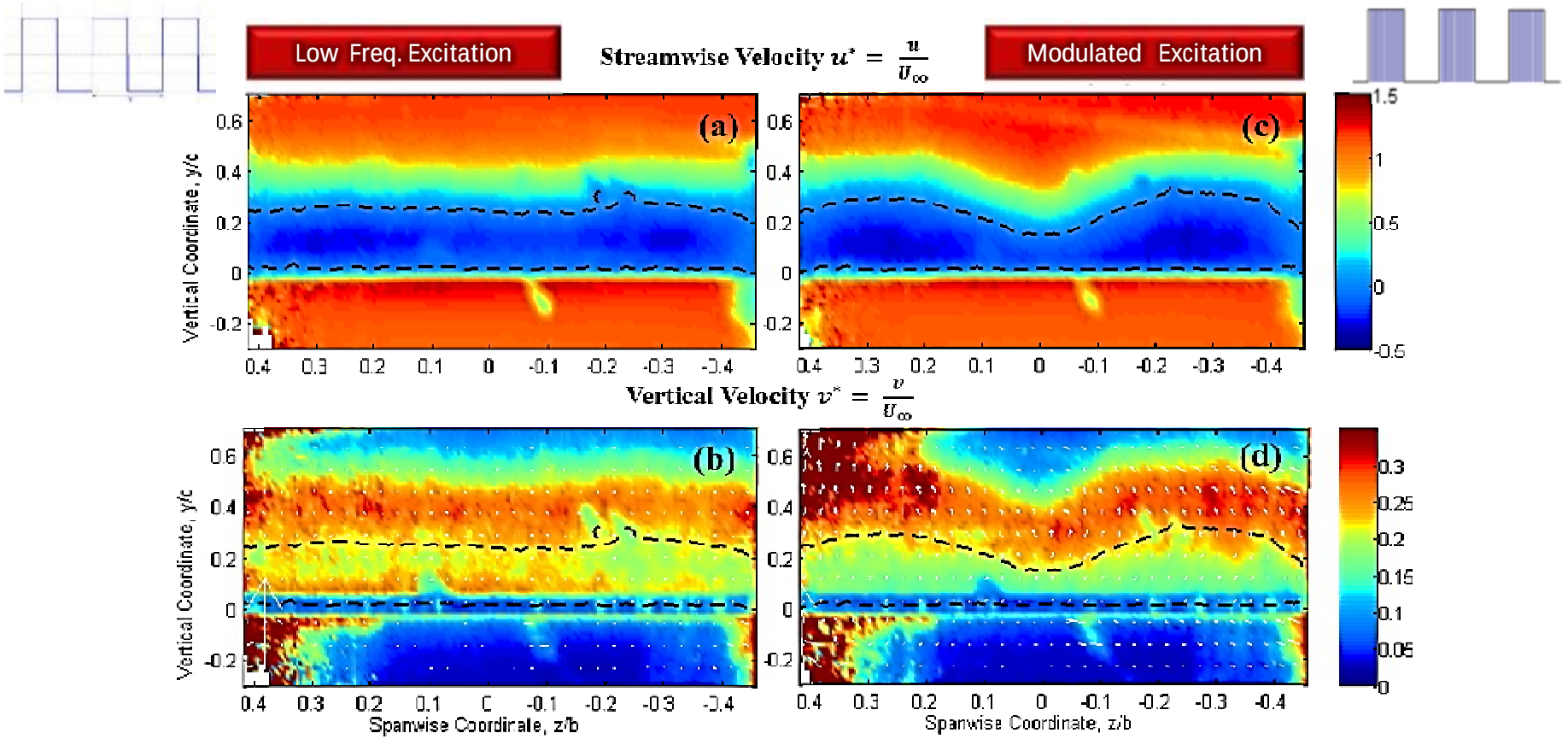

- Modulating the low-freq. signal with a high-freq. carrier wave leads to the emergence of stall cells
- The streamwise vortices are not eliminated by spanwise shedding when the signal is modulated. The shedding strength is also increased as a result of modulation.

Outline

- Previous Work/Background
- Motivation /Introduction
- Experimental Setup
- Results
  - Surface Topology (Fluorescent Surface Oil Flow Visualization)
  - Velocity Distribution (2D-2C and Stereo PIV)
- Hypothesis
- Conclusions

Waveform Modulation: Increase in Perturbation Amplitude

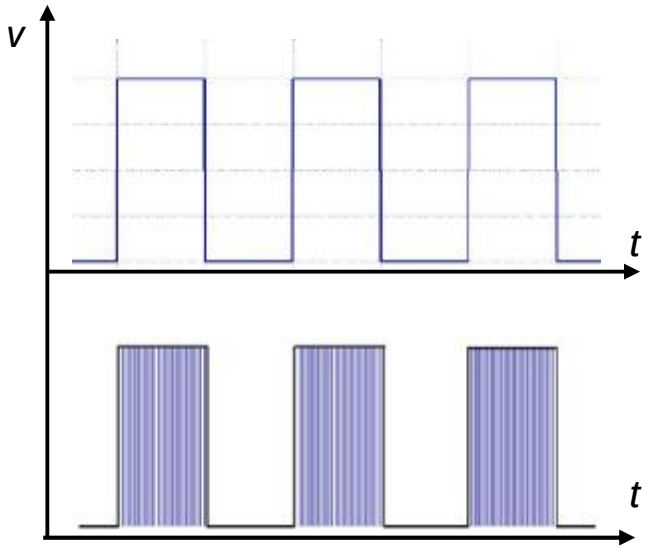

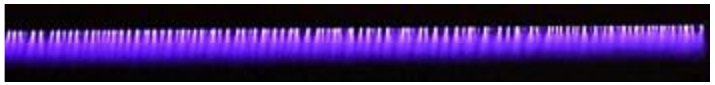

Square continuous pulse train at f_e = 110 Hz

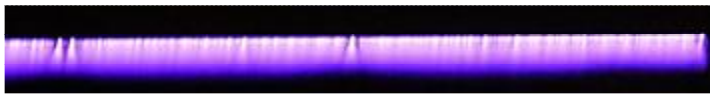

Square continuous pulse train at f_e = 110 Hz modulated by carrier wave at f_c = 2 kHz

- It is known that as the pulse repetition rate is increased, the thermal energy released after each pulse is reduced[1]. However, the total thermal energy released in a specific period of time is increased.
- The flow response to a high-freq. pulse train and a low-freq. modulated signal is quite similar as evidenced by stereo-PIV and surface pressure data
- We postulate that stall cells emerge as a result of an increase in perturbation amplitude or increase in perturbation frequency. Similar effects are also observed when the signal is modulated.

1. NETL internal report, 2015
2. Dawson, R., and Little, J., *Journal of Applied Physics*, vol. 113, Mar. 2013, p. 103302

Outline

- Previous Work/Background
- Motivation /Introduction
- Experimental Setup
- Results
  - Surface Topology (Fluorescent Surface Oil Flow Visualization)
  - Velocity Distribution (2D-2C and Stereo PIV)
- Hypothesis
- Conclusions

Conclusions:

- In contrast to the existing literature, the current results suggest that appropriate disturbance environments are conducive to the emergence of stall cells even over thin airfoils in deep stall
- Low-frequency excitation led to the emergence of well-defined spiral nodes on the airfoil surface, but a very two-dimensional flow field immediately downstream of the trailing edge. A plausible explanation is that the streamwise vortices are confined to near airfoil surface by spanwise coherent structures
- High-frequency excitation resulted in the emergence of distinct, mushroom-shaped cells over the airfoil
- These results suggest that the perturbation environment created by the NS-DBD actuators is responsible for the emergence of stall cells in flow conditions where the appearance of such features was previously believed to be unlikely
- The increase in perturbation amplitude, due to frequency increase or signal modulation, is believed to be responsible for the emergence of stall cells

THE OHIO STATE UNIVERSITY

Aerospace Research Center

Thank you for your attention

Questions?